Nuclear Engineering and Technology 52 (2020) 2949–2957

Contents lists available at ScienceDirect

Nuclear Engineering and Technology

journal homepage: www.elsevier.com/locate/net

Original Article

Crack growth analysis and remaining life prediction of dissimilar metal pipe weld joint with circumferential crack under cyclic loading

A. Ramachandra Murthy*, P. Gandhi, S. Vishnuvardhan, G. Sudharshan

CSIR-Structural Engineering Research Centre, Taramani, Chennai, 600113, India

ARTICLE INFO

Article history:
Received 24 April 2020
Received in revised form
23 May 2020
Accepted 1 June 2020
Available online 10 July 2020

Keywords:
Dissimilar metal weld joint
Piping component
Crack tip constraint
Stress intensity factor
Remaining life

ABSTRACT

Fatigue crack growth model has been developed for dissimilar metal weld joints of a piping component under cyclic loading, where in the crack is located at the center of the weld in the circumferential direction. The fracture parameter, Stress Intensity Factor (SIF) has been computed by using principle of superposition as $K_H + K_M$. K_H is evaluated by assuming that, the complete specimen is made of the material containing the notch location. In second stage, the stress field ahead of the crack tip, accounting for the strength mismatch, the applied load and geometry has been characterized to evaluate SIF (K_M). For each incremental crack depth, stress field ahead of the crack tip has been quantified by using J-integral (elastic), mismatch ratio, plastic interaction factor and stress parallel to the crack surface. The associated constants for evaluation of K_M have been computed by using the quantified stress field with respect to the distance from the crack tip. Net SIF ($K_H + K_M$) computed, has been used for the crack growth analysis and remaining life prediction by Paris crack growth model. To validate the model, SIF and remaining life has been predicted for a pipe made up of (i) SA312 Type 304LN austenitic stainless steel and SA508 Gr. 3 Cl. 1. Low alloy carbon steel (ii) welded SA312 Type 304LN austenitic stainless-steel pipe. From the studies, it is observed that the model could predict the remaining life of DMWJ piping components with a maximum difference of 15% compared to experimental observations.

1. Introduction

In nuclear industry, Dissimilar Metal Welded Joints (DMWJs) are common to join the ferritic steel pipe-nozzles of the pressure vessel to the austenitic stainless steel safe-end pipes (Fig. 1 [1]). It has been found from the literature that due to environmental conditions, thermal loading, over loading, ageing etc., crack may initiate at any of the critical locations such as in the weld, heat affected zone, base metal etc. [2–5]. Scott et al. [6] carried out fracture studies on two bi-metallic specimens made up of ferritic cold-leg pipe (A516 Gr. 70) and stainless-steel pipe (SA182 F316) joined by Inconel 182 weld rod as filler material. Burstow et al. [7] performed a two-dimensional finite element analysis using the modified boundary layer formulation to quantify the influence of constraint on crack tip stress fields in strength mismatched welded joints.

Østby et al. [8] studied the change in near-tip stress field in small scale yielding for cracks located at an interface between two materials with different plastic work hardening. Two major multi-partner projects, mainly funded by industry and partly by the European Commission, were on structural integrity of Bi-Metallic Welds (BMW) namely BIMET [9–12]. All the tests were performed on four-point bend specimens, made up of A508 low alloy steel and 304LN austenitic stainless steel. For the weld and buttering, 308L/309L were used. Structural integrity assessment of these piping components is of paramount importance for design and safety management of nuclear power plants. Due to highly inhomogeneous nature across dissimilar metal weld joints in terms of mechanical, fracture and thermal, only few investigations were reported at coupon/specimen levels [13,14].

Deng et al. [15] proposed a simplified methodology to compute residual stresses in a dissimilar metal pipe joint accounting cladding, buttering, post weld heat treatment and multi-pass welding using a united approach. Deng et al. [16] performed both numerical simulation and experiments to investigate welding residual stress distribution in a dissimilar metal pipe joint. Zhao et al. [17] investigated the characteristics of residual stresses on the dissimilar welded pipe between T92 steel and S30432 steel by using finite element method. The aspects such as the effects of heat input,

* Corresponding author.
E-mail addresses: murthyarc@serc.res.in (A.R. Murthy), svvardhan@serc.res.in (S. Vishnuvardhan).

https://doi.org/10.1016/j.net.2020.06.001

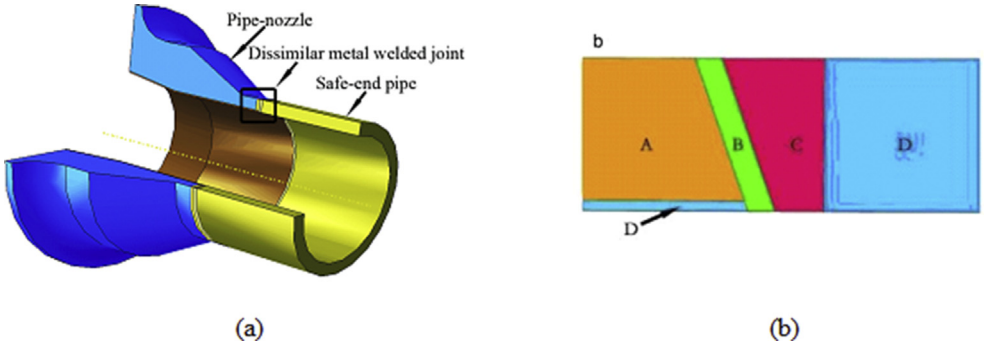

Fig. 1. A typical dissimilar metal welded joint (DMWJ) a) four materials composed of DMWJ (b) A-Ferritic steel, B- buttering alloy 82, C- weld alloy 182, D- Austenitic stainless steel 316L.

groove shape and layer number on the residual stress distribution were studied. Wang et al. [1] conducted fracture and microscopic tests on an Alloy52 M dissimilar metal welded joint between A508 ferritic steel and 316LN stainless steel to understand the fracture mechanism of different regions within the joint. It was noticed from their study that the fracture mechanism of A508 and 316LN base metals and heat-affected-zone of 316LN is a ductile mode of fracture. Bin Wang et al. [18] performed experiments on bimetallic composite pipe welded joint and microstructure studies. A characterization method based on the electron backscatter diffraction technique was proposed to analyse the features of grain and microstructure within crack site. Kumar et al. [19] evaluated the local tensile and fracture toughness properties of the dissimilar metal weld joints between SA508 Gr.3 Cl.1 and SA312 Type 304LN pipe. Specimens were extracted from different regions of dissimilar metal weld such as heat affected zones, fusion lines, buttering layer, weld metal and both base metals to study the local tensile and fracture toughness. The results were substantiated through metallurgical and fracture surface investigations. Recently, Murthy et al. [20] and Kumaran et al. [21] carried out numerical fracture studies on specimens (uniaxial tension and three-point bend) made up of dissimilar metal weld. It was observed from the uniaxial tension studies that (i) SIF increases with increase of crack length and DMWJ (ii) SIF of DMP reduces compared to homogenous plate (iii) constraint effect is found to be significant, if DMWJ is less than the initial crack length, resulted in reduction of SIF (iv) constraint effect is found to be insignificant if DMWJ is more than 20 mm and the ratio of crack length to DMWJ is greater than 0.75. Further, it was observed from the studies on dissimilar metal Single Edged Notch Bending (DMSENB) specimens that (i) SIF increases with increase of crack length and DMWJs (ii) significant constraint effect (geometry, crack tip and strength mismatch) was observed for DMWJs of 5 mm and 10 mm (iii) stress distribution at the interfaces of DMSENB specimen exhibits clear indication of strength mismatch (iv) constraint effect was found to be significant if DMWJ was less than 20 mm and the ratio of specimen length to the DMWJ was greater than 7.4 [1].

Since, the piping components of nuclear industry are ductile in nature, the failure is accompanied by crack initiation and crack propagation. Hence, leak-before-break concepts can be employed for structural integrity evaluation of piping component. From the above, it can be observed that the studies carried out on structural components made up of DMWJ are scanty. In view of this, a fatigue crack growth model has been developed for DMWJ piping components considering the constraint effects.

2. Development of fatigue crack growth model

To develop a fatigue crack growth model, it is essential to determine a reliable fracture parameter, namely, stress intensity factor. The cracks are assumed to be within the material and propagate parallel to material interface. Crack propagation in welded joints is also significantly influenced by the fracture toughness and yield strength of the constituent materials. Understanding the effects of strength mismatching and geometry on the behaviour of the materials surrounding a crack is essential for accurate estimation of fracture parameter which in turn will be useful for crack growth analysis and remaining life prediction. The variation in crack tip stress field due to geometrical constraint and strength mismatch can be modelled by varying the magnitude of the T-stress and strength of the base material outside the weld respectively [7].

The net Stress Intensity Factor (SIF) for dissimilar metal weld joints of a piping component under cyclic loading has been computed by using principle of superposition as:

$$K_{NET} = K_H + K_M \tag{1}$$

2.1. Determination of K_H

K_H is evaluated by assuming that, the complete specimen is made of the material containing the notch location. Although, several methods are available to evaluate SIF (K_H), RCC-MR approach has been followed in the present study. Brief details about RCC-MR are given below [22]. SIF for the case of piping component with part through external crack is given by (Fig. 2).

$$K_I = \left\{\sigma_0 i_0 + \sigma_1 i_1\left(\frac{a}{t}\right) + \sigma_{gb}F_{gb}\right\}\sqrt{\pi a} \text{ for the deepest point} \tag{2}$$

$$K_I = \left\{\sigma_0 i_0 + \sigma_1 i_1\left(\frac{a}{t}\right) + \sigma_{gb}F_{gb}\right\}\sqrt{\pi c} \text{ for the surface point} \tag{3}$$

Where,

$$\sigma_0 = \left\{\frac{N_1}{\pi\left(r_e^2 - r_i^2\right)} + P\left(\frac{r_e^2}{r_e^2 - r_i^2}\right) + \frac{E\alpha\theta_1}{2(1-\vartheta)} \times \frac{2r_i}{3h}\left[\frac{2r_e^2}{r_i(r_e + r_i)} - 1\right]\right\} \tag{4}$$

$$\sigma_1 = -\frac{E\alpha\theta_1}{2(1-\vartheta)} \tag{5}$$

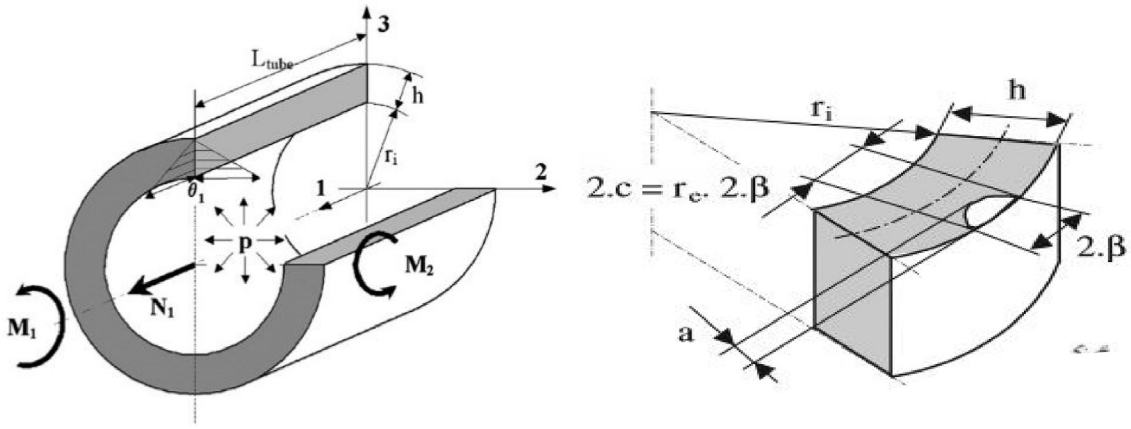

Fig. 2. Schematic diagram of piping component with part-through crack configuration.

$$\sigma_{gb} = \frac{M_2 r_e}{(\pi/4)\left(r_e^4 - r_i^4\right)} \tag{6}$$

Where, r_i, r_e and r_m = internal, external and average radius respectively; h and L_{tube} = thickness and length of the tube; a, 2c and 2β = depth, length and angle (in radians) of the defect respectively with symmetrical position in relation to the bending plane; P= Internal pressure; M_1=Torsion moment along axis 1; M_2 = Global bending moment along axis 2; ϕ_1 and ϕ_2 = Rotation of the section around axis 1 and 2 respectively; N_1 = Axial load (Without pressure effect on the end closure; u1 = axial elongation; θ_1 = linear temperature gradient; $F_{gb\ deep}$ = Geometric factor at the deepest point of crack depth; $\sigma_{gb\ max}$ and $\sigma_{gb\ min}$ = Maximum and minimum global bending stress respectively.

In this present study, experimental investigations have been carried out on pipes under four-point bending. Hence, the above equations are simplified as: SIF at deepest point:

$$SIF_{Max} = \left(F_{gb\ deep}\sigma_{gb\ max}\right)\sqrt{\pi a} \tag{7}$$

$$SIF_{Min} = \left(F_{gb\ deep}\sigma_{gb\ min}\right)\sqrt{\pi a} \tag{8}$$

$$\sigma_{gb\ max} = \frac{M_{max} r_e}{(\pi/4)\left(r_e{}^4 - r_i{}^4\right)} \tag{9}$$

$$\sigma_{gb\ min} = \frac{M_{min} r_e}{(\pi/4)\left(r_e{}^4 - r_i{}^4\right)} \tag{10}$$

2.2. Determination of K_M

In second stage, the stress field ahead of the crack tip, accounting for the strength mismatch, the applied load and geometry has been characterized to evaluate SIF (K_M). For each incremental crack depth, stress field ahead of the crack tip has been quantified by using J-integral (elastic), strength mismatch ratio, plastic interaction factor and stress parallel to the crack surface [23]. The associated constants for evaluation of K_M have been computed by using the quantified stress field with respect to the distance from the crack tip [24].

The existing standards have been modified to account for the influence of stress triaxiality in the flaw assessment procedures. These modifications are based on the ability of so called 'constraint parameters' to describe the near tip stresses. Crack tip stresses in homogeneous fracture specimens are successfully described in terms of two parameters like J-Q or K-T [25,26].

In a cylindrical coordinate system (r, θ), the crack tip stress (σ_{ij}) can be characterized as:

$$\sigma_{ij} = \frac{K_I}{\sqrt{2\pi r}} f_{ij}(\theta) + T_{1I}\partial_{1i}\partial_{1j} \tag{11}$$

Where, K_I is the elastic stress intensity factor and T_{1I} is a stress parallel to the crack.

For fracture specimens having crack at weld center, strength mismatch ratio between base and weld material and weld width are the additional variables, along with the magnitude of applied loading, type of loading, and geometry of specimen that affect the crack tip stresses [23].

An alternative method of quantifying constraint effects on crack tip stress fields is the Q-stress parameter. This seeks to describe the deviation of the stress field from that predicted from the HRR field [27,28], which describes the crack tip stress distribution in terms of the magnitude of the elastic-plastic J-parameter [25,26]. A scheme was proposed by Kumar et al. [23] involving the mismatch ratio and plastic interaction factor. They showed that the crack tip stress fields can be described as being of the form:

$$\left(\frac{\sigma_{yy}}{\sigma_0}\right)_M = \left(\frac{\sigma_{yy}}{\sigma_0}\right)_{M=1,T=0} + Q + (1-M)\left(aI_p{}^2 + b\right)\frac{r}{\frac{J}{\sigma_0}} \tag{12}$$

For $2 \le \frac{r}{\frac{J}{\sigma_0}} \le 5$

Where, the first term represents the crack tip opening stress for a homogeneous cracked specimen under the Small-Scale Yielding (SSY). It is defined as [29]:

$$\left(\frac{\sigma_{yy}}{\sigma_0}\right)_{M=1,T=0} = \left(\frac{J}{\alpha\varepsilon_0\sigma_0 I_n r}\right)^{\frac{1}{n+1}} \widetilde{\sigma_{ij}(\theta, n)} \tag{13}$$

$$J = J_{el} = \frac{K_H{}^2}{E}\left(1-\mu^2\right) \tag{14}$$

Where, J_{el} (elastic J −integral) for plane strain; ε_0 and σ_0 are constants in the power-law plasticity constitutive equation; n is the material hardening exponent; α and I_n are constants.

$I_n = 10.4\sqrt{0.13+n} - 4.8n$, n = strain hardening exponent

r = distance from the crack tip

$$I_p = \frac{4\frac{J}{h\sigma_0}}{\left(\frac{T}{\sigma_0} + \sqrt{4-(3-4\mu^2)\left(\frac{T}{\sigma_0}\right)^2}\right)^2} \quad (16)$$

α, $\sigma_{ij}(\check{\theta}, n)$ constants tabulated by Shih in Tables of HRR singular field quantities

σ_0 = Yield strength of the weld

The second term Q is defined as a triaxiality parameter and it parameterizes the strain field when distances ahead of the crack front are normalized by J/σ_0. It is defined as:

$$Q = \frac{\sigma_{yy} - (\sigma_{yy})_{SSY;T=0}}{\sigma_0} at\ \ \theta = 0, r = \frac{2J}{\sigma_0} \quad (15)$$

A negative Q value means the hydrostatic stress is lower than the reference yield stress and vice-versa.

The third term accounts for the effect of constraint developed due to weld strength mismatch. It comprises of weld mismatch ratio (M) and a plastic interaction factor (I_p) that scales the size of plastic zone with half of the weld width. The extent of penetration of the plastic zone in the base material governs the degree of influence of weld strength mismatch on crack tip stress. It is defined as follows:

Where, $M = \frac{\sigma_{0W}}{\sigma_{0B}} = \frac{\text{Yield strength of weld material}}{\text{Yield strength of Base material}}$,
a, b = constants evaluated based on n,
starin hardening coefficient T = T – stress, μ = Poisson's ratio, SIF (K_M) can be calculated from Williams et al. [24] by substituting the calculated stress tensor in the following equation,

$$\sigma_x = \sum_{n=1}^{\infty} \frac{n}{2} r^{\frac{n}{2}-1} a_n \Big[\times \left(2+\frac{n}{2}+(-1)^n\right)\cos\left(\frac{n}{2}-1\right)\theta - \left(\frac{n}{2}-1\right)\cos\left(\frac{n}{2}-3\right)\theta\Big] \quad (17)$$

$$\sigma_y = \sum_{n=1}^{\infty} \frac{n}{2} r^{\frac{n}{2}-1} a_n \Big[\times \left(2-\frac{n}{2}-(-1)^n\right)\cos\left(\frac{n}{2}-1\right)\theta + \left(\frac{n}{2}-1\right)\cos\left(\frac{n}{2}-3\right)\theta\Big] \quad (18)$$

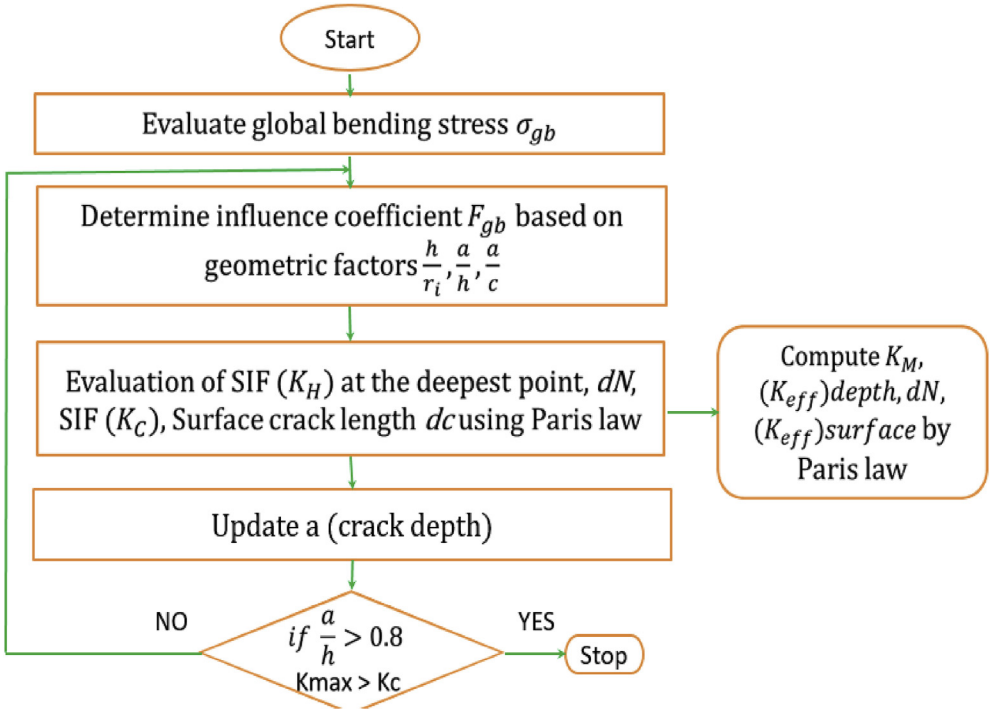

Fig. 3. Sequential steps to develop a fatigue crack growth model for DMWJ pipes.

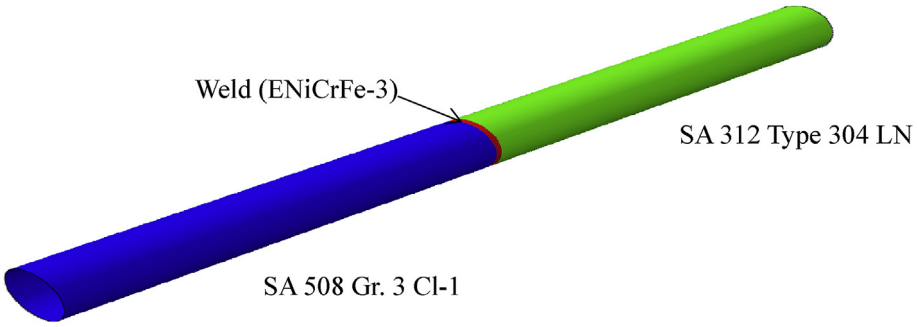

Fig. 4. Schematic diagram of bi-metallic pipe weld joint.

Table 1
Geometrical configuration of bi-metallic pipe.

Pipe (DW-C-1)			Notch			
L mm	D	t	2C mm	W	a	2θ degrees
4012	324	24	63	3	6.51	22.58

Table 2
Mechanical properties of bi-metallic pipe.

Material	σ_y, MPa	σ_u, MPa	Elongation, %	E, GPa
SA 508 Gr. 3 Cl-1	570	694	23	227
SA 312 Type 304LN	208	549	81	194

Fig. 5. Final deflected shape of the pipe.

$$\tau_{xy} = \sum_{n=1}^{\infty} \frac{n}{2} r^{\frac{n}{2}-1} a_n \Big[\times \left(\frac{n}{2}-1\right)\sin\left(\frac{n}{2}-3\right)\theta - \left(\frac{n}{2}+(-1)^n\right)\sin\left(\frac{n}{2}-1\right)\theta \Big] \quad (19)$$

Where the coefficient a_1 is determined and subsequently the SIF,

$$K_{Mx} = a_1\sqrt{2\pi}, K_{My} = a_1\sqrt{2\pi}, K_{Mxy} = a_1\sqrt{2\pi} \quad (20)$$

The resultant SIF is determined by,

$$K_M = \sqrt[2]{{K_{Mx}}^2 + {K_{My}}^2 + K{K_{Mxy}}^2} \quad (21)$$

Fig. 6. Close-up view of crack location.

Table 3
Geometrical configuration of SA312 Type 304LN stainless steel pipe.

Pipe			Notch			
L mm	D	t	2C mm	W	a	2θ degrees
2518	170	14.55	7	2	3.42	4.72

2.3. Prediction of remaining life

The Paris law is then used to predict the remaining life of the specimen. For each incremental depth, the corresponding change in surface crack length is also calculated by using the same law, and it is iterated till the depth reaches 0.8 times the thickness of the pipe.

$$\frac{da}{dN} = C(\Delta K)^m \quad (22)$$

Where, C and m – Crack growth constants; $\Delta K(K_{max} - K_{min})$ –effective SIF; $\frac{da}{dN}$ – Crack growth rate in mm/cycle.

Table 4
Mechanical properties of SA 312 Type 304LN stainless steel pipe.

Material	σ_y, MPa	σ_u, MPa	Elongation, %	E, GPa
SA 312 Type 304LN	208	549	81	194

Fig. 3 presents the typical flowchart containing sequential steps for development of a fatigue crack growth model for dissimilar metal weld piping components.

3. Validation studies

3.1. Details of piping components

Case 1. Crack growth analysis and remaining life prediction of bi-metallic pipe weld joint (SA 508 Gr. 3 Cl-1 and SA 312 Type 304LN)

The materials used in bi-metallic pipe weld joints are SA 508 Gr. 3 Cl-1 (low alloy carbon steel or ferritic) and SA 312 Type 304LN (stainless steel or austenitic). The weld joint was prepared using consumable of Nickel based alloy (ENiCrFe-3) (Fig. 4). Thickness of ferritic and austenitic pipes is 24.5 and 23.9 mm respectively. So, the thickness of pipe is considered as 24 mm. Specimen contains part-through notch and is located at the centre of the weld. Geometrical configuration and material properties of bi-metallic pipe are given in Tables 1 and 2 respectively. The initial notch profile was semi-elliptical and the notch tip radius was 0.1 mm. Bi-metallic pipe weld joint is subjected to cyclic load with a stress ratio of 0.1 and the frequency is maintained in the range of 0.5–1.0 Hz during experimentation. The maximum amplitude is 480 kN. Where, L –Length; D-Diameter; t-thickness; 2C, W, a and 2θ – length, width, initial depth and initial angle of the notch.Where, σ_y - Yield strength; σ_u - Ultimate tensile strength; E– Young's modulus.

The final deflected shape of the pipe and the close-up view of crack locations are shown in Figs. 5 and 6 respectively [30].

Case 2. Crack growth analysis and remaining life prediction of SA312 Type 304LN austenitic stainless steel pipe weld joint

To further validate the model, SIF and remaining life has been predicted for a pipe made up of SA312 type 304LN austenitic stainless steel connected by a weld. Geometrical configuration and material properties of SA312 Type 304LN stainless steel pipe are given in Tables 3 and 4 respectively. Four point bending is carried out under load control. Inner and outer span of the pipe are 680 mm and 1700 mm respectively. The initial notch profile was semi-elliptical and the notch tip radius was 0.1 mm. Cyclic load is applied with a stress ratio of 0.1 and the frequency is maintained in the range of 0.5–2.0 Hz during experimentation. The maximum amplitude is 258 kN.

3.2. Results and discussions on fatigue crack growth model implementation

Case 1 Crack growth analysis and remaining life prediction of bi-metallic pipe weld joint (SA 508 Gr. 3 Cl-1 and SA 312 Type 304LN)

Initially, homogenous material made up of weld (ENiCrFe-3) is taken for the analysis described in Section 2.1. In the second stage (section 2.2), the crack tip stress field developed ahead of the crack tip in a Bi-metallic pipe specimen involving the additional constraint parameters such as weld strength mismatch and weld width are evaluated. J-integral ($J_{elastic}$) is determined corresponding to SIF (K_H) for each incremental crack depth and the associated constants are evaluated in calculating the crack tip stress field. Fig. 7 shows the stress field variation ahead of the crack tip accounting for constraint parameters Q and T. Finally, the additional stress intensity factor has been evaluated by substituting the evaluated stress value in the corresponding stress tensor expression. The process is repeated for each constant incremental crack depth and it concludes, when the crack depth has attained 80% of the thickness of the bi-metallic pipe weld joint. Now, for the crack growth analysis, the number of cycles required for the crack depth to reach the next increment value is determined using the Paris law. For each incremental crack depth, corresponding change in surface crack length is then determined.

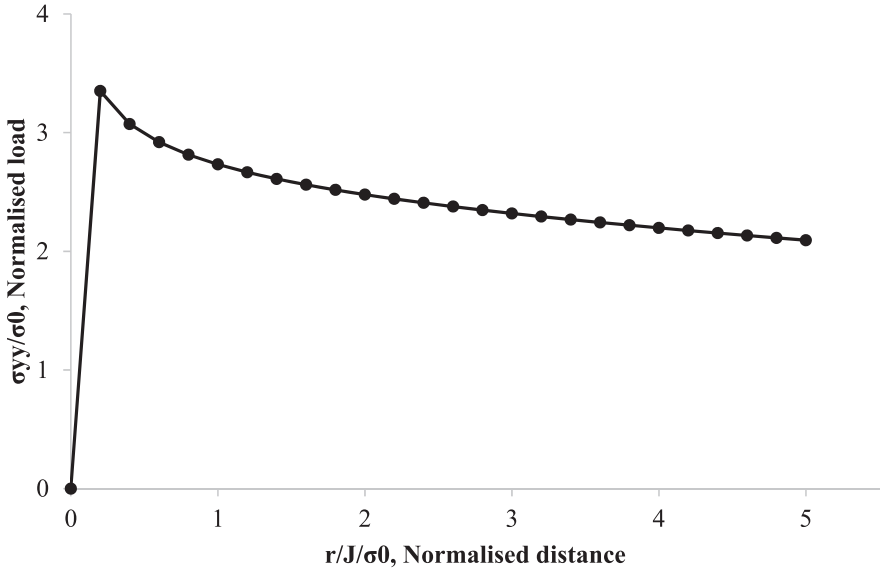

Fig. 7. Crack tip stress field for typical SIF.

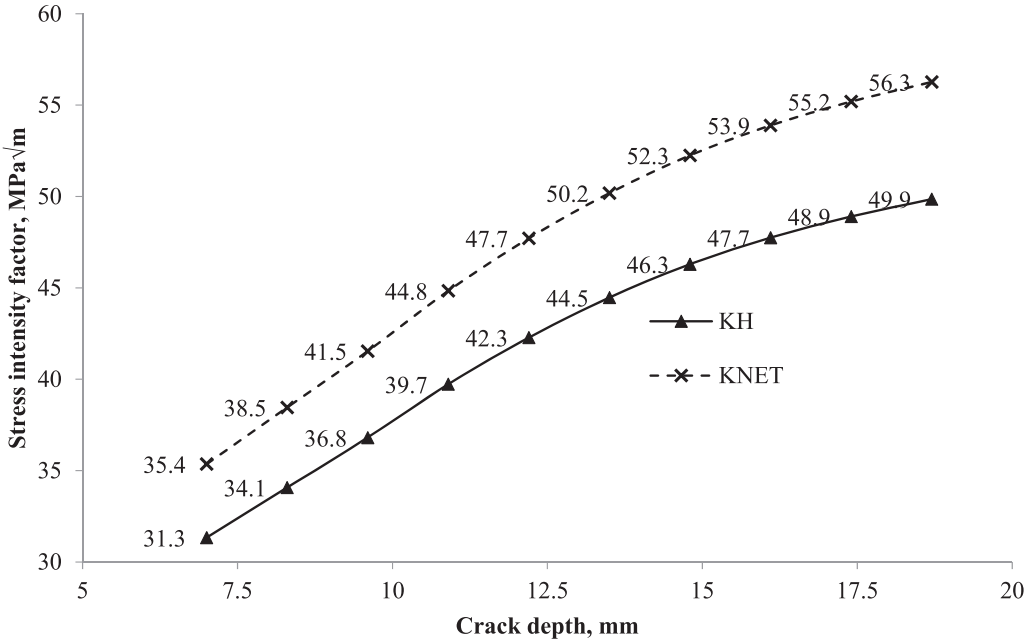

Fig. 8. Stress intensity factor vs crack depth.

Fig. 8 exhibits the stress intensity factor vs crack depth. From Fig. 8, it can be clearly observed that the amount of energy required to propagate the crack growth in the bi-metallic piping component is lower than the homogenous. Since, the K_H and K_{NET} could represent the SIF of homogenous and bi-metallic pipe respectively.

Fig. 9 shows the crack depth vs number of cycles to failure and it resulted that the high number of cycles for homogenous case which has the similarity to Fig. 8 with respect to the failure. It can be clearly seen that the predicted remaining life with net SIF is in good agreement with the corresponding experimental observations. The percentage difference between experimental and predicted life is about 6%. Further, it can be observed from Fig. 9 that the predicted remaining life with SIF (K_H) is significantly higher (about 30%) compared to experimental observations.

Case 2 Crack growth analysis and remaining life prediction of SA312 Type 304LN austenitic stainless steel pipe weld joint

From Fig. 10 (Crack depth vs number of cycles), it can be noted that the number of cycles predicted for stainless steel pipe weld joint with K_{net} is 409884 and with K_H is 573565 cycles. The corresponding experimental value is 422909 cycles. It can be clearly seen that the predicted remaining life with net SIF is in good agreement with the corresponding experimental observations. The percentage

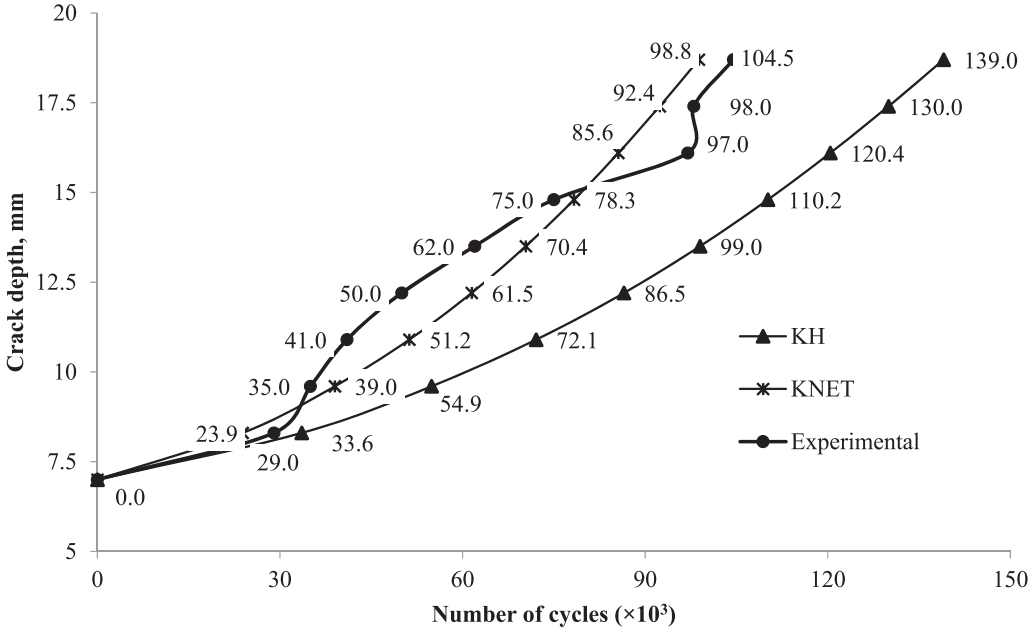

Fig. 9. Crack depth vs number of cycles.

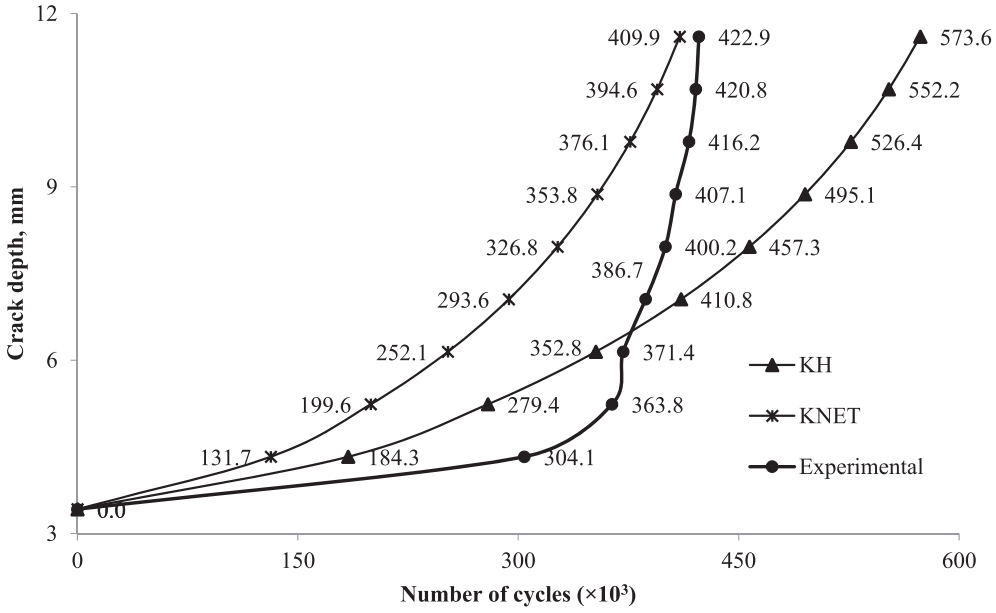

Fig. 10. Crack depth vs number of cycles.

difference between experimental and predicted life with K_{net} is about 5%. Further, it can be observed from Fig. 10 that the predicted remaining life with SIF (K_H) is significantly higher (about 35%) compared to experimental observations.

4. Summary

For structural integrity assessment of dissimilar metal weld joint of piping components, crack growth analysis and remaining life is essential. In view of this, a fatigue crack growth model has been developed for a piping component with narrow groove girth weld under cyclic loading, where in the crack is located at the center of the weld in the circumferential direction. The fracture parameter, stress intensity factor (SIF) has been determined in two stages. In first stage, SIF is determined for the specimen assuming that, the complete specimen is made of the material containing the notch location (K_H). In second stage, the stress field ahead of the crack tip, accounting for the strength mismatch, the applied load and geometry has been characterized to evaluate SIF (K_M). For each incremental crack depth, stress field ahead of the crack tip has been quantified by using J-integral (elastic), mismatch ratio, plastic interaction factor and stress parallel to the crack surface. The associated constants for evaluation of K_M have been computed by using the quantified stress field with respect to the distance from the crack tip. Net SIF ($K_H + K_M$) computed, along with the established Paris crack growth model has been used for the crack growth analysis and remaining life prediction. To validate the model, SIF and remaining life has been predicted for a pipe made up of (i) SA 508 Gr. 3 Cl-1 low alloy carbon steel and SA 312 Type 304LN stainless steel joined by weld (ii) SA312 Type 304LN austenitic stainless steel joined by weld. From the model, it is found that the predicted remaining life with net SIF is in good agreement with the corresponding experimental observations. The percentage difference between experimental and predicted life with net SIF is about 5%. Further, it is found from that the predicted remaining life with SIF (K_H) is significantly higher (30–35%) compared to corresponding experimental observations.

Declaration of competing interest

The authors declare that they have no known competing financial interests or personal relationships that could have appeared to influence the work reported in this paper.

References

[1] H.T. Wang, G.Z. Wang, F.Z. Xuan, S.T. Tu, Fracture mechanism of a dissimilar metal welded joint in nuclear power plant, Eng. Fail. Anal. 28 (2013) 134–148, https://doi.org/10.1016/j.engfailanal.2012.10.005.
[2] PWR Material Realiability Project, Interim Alloy 600 Safety Assessment for U.S. PWR Plants, Part 1: Alloy82/182 Pipe Butt Welds, EPRI Report TP-1001491, 2001.
[3] R. Celin, F. Tehovnik, Degradation of a Ni-Cr-Fe alloy in a pressurised water nuclear power plant, Mater. Technol. 45 (2011) 151–157.
[4] A. Jenssen, K. Norrgard, J. Lagerstron, Assessment of cracking in dissimilar metal welds. Proc. Of Tenth Int. Symp. on Environmental Degradation of Materials in Nuclear Power Systems-Water Reactors, NACE International, USA, 2001. CD-ROM.
[5] S. Farley, An overview of non destructive inspection service in nuclear power plants. International Conference on Nuclear Energy for New Europe, Portoraz, Slovenia, 2004.
[6] P. Scott, R. Francini, S. Rahman, A. Rosenfield, G. Wilkowski, Fracture Evaluations of Fusion Line Cracks in Nuclear Pipe Bimetallic Welds. NUREG/CR-6297, U.S. Nuclear Regulatory Commission, Washington, DC, 1995, https://doi.org/10.2172/53643.
[7] M.C. Burstow, I.C. Howard, R.A. Ainsworth, The influence of constraint on crack tip stress fields in strength mismatched welded joints, J. Mech. Phys. Solid. 46 (5) (1998) 845–872, https://doi.org/10.1016/S0022-5096(97)00098-7.
[8] E. Østby, Z.L. Zhang, C. Thaulow, Constraint effect on the near tip stress fields due to difference in plastic work hardening for bi-material interface cracks in small scale yielding, Int. J. Fract. 111 (2001) 87–103, https://doi.org/10.1023/A:1010992906312.
[9] G. Chas, C. Faidy, R. Hurst, Sructural integrirt of bi-metallic wlds in piping: fracture testing and analysis, in: ASME 2001 Pressure Vessels and Piping Conference (PVP 2001), Atlanta, USA, vol. 423, 2001, July, 22-26.
[10] Karl-Heinz Schwalbea, Alfred Corneca, David Lidbury, Fracture mechanics analysis of BIMET welded pipe tests, Int. J. Pres. Ves. Pip. 81 (3) (2004) 251–277, https://doi.org/10.1016/j.ijpvp.2003.12.016.
[11] C. Faidy, Structural Integrity of Dissimilar Welds: ADIMEW Project Overview. Flaw Evaluation, Service Experience, and Materials for Hydrogen Service, 2004, https://doi.org/10.1115/pvp2004-2540.
[12] G. Martin, A. Menard, Experimental four point bending test on a real size bimetallic welded pipe: European project ADIMEW. In: ASME 2004 Pressure Vessels and Piping Conference (PVP 2004), San Diego, USA, 2004, July, 25-29.

[13] C. Jang, J. Lee, J.S. Kim, Mechanical property variation within Inconel 82/182 dissimilar metal weld between low alloy steel and 316 stainless steel, Int. J. Pres. Ves. Pip. 85 (2008) 635–646, https://doi.org/10.1016/j.ijpvp.2007.08.004.
[14] J.W. Kim, K. Lee, J.S. Kim, Local mechanical properties of Alloy 82/182 dissimilar weld joint between SA508 Gr.1a and F316 SS at RT and 320°C, J Nual Mater 384 (2009) 212–221, https://doi.org/10.1016/j.jnucmat.2008.11.019.
[15] Dean Deng, Kazuo Ogawa, Shoichi Kiyoshima, Nobuyoshi Yanagida, Koichi-Saito, Prediction of residual stresses in a dissimilar metal welded pipe with considering cladding, buttering and post weld heat treatment, Comput. Mater. Sci. 47 (2) (2009) 398–408, https://doi.org/10.1016/j.commatsci.2009.09.001. December 2009.
[16] Dean Deng, Shoichi Kiyoshima, Kazuo Ogawa, Nobuyoshi Yanagida, Koichi Saito, Predicting welding residual stresses in a dissimilar metal girth welded pipe using 3D finite element model with a simplified heat source, Nucl. Eng. Des. 241 (1) (2011) 46–54, https://doi.org/10.1016/j.nucengdes.2010.11.010. January 2011.
[17] Lei Zhao, Jun Liang, Qunpeng Zhong, Chao Yang, Biao Sun, Jinfeng Du, Numerical simulation on the effect of welding parameters on welding residual stresses in T92/S30432 dissimilar welded pipe, Adv. Eng. Software 68 (2014) 70–79, https://doi.org/10.1016/j.advengsoft.2013.12.004. February 2014.
[18] Bin Wang, Bo-bo, Wei Lei, Ming Wang, Xu Liang Wang, Investigations on the crack formation and propagation in the dissimilar pipe welds involving L360QS and N08825, Eng. Fail. Anal. 58 (1) (2015) 56–63, https://doi.org/10.1016/j.engfailanal.2015.08.034. December 2015.
[19] S. Kumar, P.K. Singh, K.N. Karn, V. Bhasin, Experimental investigation of local tensile and fracture resistance behaviour of dissimilar metal weld joint: SA508 Gr.3 Cl.1 and SA312 Type 304LN, Fatig. Fract. Eng. Mater. Struct. (2016), https://doi.org/10.1111/ffe.12484.
[20] A. Ramachandra Murthy, M. Muthu Kumaran, M. Saravanan, P. Gandhi, Effect of dissimilar metal SENB specimen width and crack length on stress intensity factor, Nuclear Engineering and Technology (2019), https://doi.org/10.1016/j.net.2019.12.018.
[21] Kumaran M. Muthu, A. Ramachandra Murthy, S. Vishnuvardhan, Effect of constraints on stress intensity factor for dissimilar metal plate with centre crack under uniform tension, Materials Today Communications 22 (2020), 100807, https://doi.org/10.1016/j.mtcomm.2019.100807, 2020.
[22] S. Marie, S. Chapuliot, Y. Kayser, M.H. Lacire, B. Drubay, B. Barthelet, P. Le Delliou, V. Rougier, C. Naudin, P. Gilles, M. Triay, French RSE-M and RCC-MR code appendices for flaw analysis: presentation of the fracture parameters calculation-Part III: cracked pipes, Int. J. Pres. Ves. Pip. 84 (2007) 614–658, https://doi.org/10.1016/j.ijpvp.2007.05.003.
[23] Suranjit Kumar, I.A. Khan, V. Bhasin, R.K. Singh, Characterization of crack tip stresses in plane-strain fracture specimens having weld center crack, Int. J. Solid Struct. 51 (2014) 1464–1474, https://doi.org/10.1016/j.ijsolstr.2013.12.039.
[24] M.L. Williams, Pasadena, and Calif, On the stress distribution at the base of a stationary crack, J. Appl. Mech. 24 (1) (1956) 109–114.
[25] N.P. O'Dowd, C.F. Shih, Family of crack tip fields characterized by a triaxiality parameter. I: structure of field, J. Mech. Phys. Solid. 39 (1991) 898–1015, https://doi.org/10.1016/0022-5096(91)90049-T.
[26] N.P. O'Dowd, C.F. Shih, Family of crack tip fields characterized by a triaxiality parameter. II: structure of field, J. Mech. Phys. Solid. 40 (1992) 939–963, https://doi.org/10.1016/0022-5096(92)90057-9.
[27] J.W. Hutchinson, Singular behaviour at the end of a tensile crack in a hardening material, J. Mech. Phys. Solid. 16 (1968) 13–31, https://doi.org/10.1016/0022-5096(68)90014-8.
[28] J.R. Rice, G.F. Rosengren, Plane strain deformation near a crack tip in a power law hardening material, J. Mech. Phys. Solid. 16 (1968) 1–12, https://doi.org/10.1016/0022-5096(68)90013-6.
[29] S.J. Hudak, R.J. Bucci, Fatigue Crack Growth Measurement and Data Analysis, vol. 738, ASTM Special Technical Publication, 1981.
[30] M. Saravanan, S. Vishnuvardhan, A. Ramachandra Murthy, P. Gandhi, Punit Arora, Suranjit Kumar, P.K. Singh, Fatigue crack growth and fracture studies on bi-metallic pipe weld joints having circumferential part-through notch in the weld. Proceedings of the 3rd International Conference & Exhibition on Fatigue, Durability and Fracture Mechanics, Belagavi, India, 2019. August 29-31, 2019.